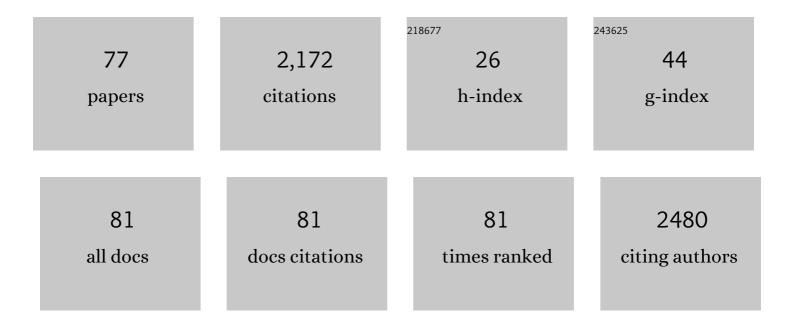
List of Publications by Year in descending order

Source: https://exaly.com/author-pdf/7260619/publications.pdf Version: 2024-02-01



#	Article	IF	CITATIONS
1	Structure of the Human Cytomegalovirus Protease Catalytic Domain Reveals a Novel Serine Protease Fold and Catalytic Triad. Cell, 1996, 86, 835-843.	28.9	171
2	Structural basis of actin recognition and arginine ADP-ribosylation by <i>Clostridium perfringens</i> ι-toxin. Proceedings of the National Academy of Sciences of the United States of America, 2008, 105, 7399-7404.	7.1	104
3	Crystal structure of human D-amino acid oxidase: Context-dependent variability of the backbone conformation of the VAAGL hydrophobic stretch located at thesi-face of the flavin ring. Protein Science, 2006, 15, 2708-2717.	7.6	102
4	Crystal Structure and Site-directed Mutagenesis of Enzymatic Components from Clostridium perfringens lota-toxin. Journal of Molecular Biology, 2003, 325, 471-483.	4.2	94
5	Structural Basis of the Influenza A Virus RNA Polymerase PB2 RNA-binding Domain Containing the Pathogenicity-determinant Lysine 627 Residue. Journal of Biological Chemistry, 2009, 284, 6855-6860.	3.4	86
6	Structural Basis of the Sphingomyelin Phosphodiesterase Activity in Neutral Sphingomyelinase from Bacillus cereus. Journal of Biological Chemistry, 2006, 281, 16157-16167.	3.4	82
7	Inhibition Mechanism of Cathepsin L-Specific Inhibitors Based on the Crystal Structure of Papain–CLIK148 Complex. Biochemical and Biophysical Research Communications, 1999, 266, 411-416.	2.1	81
8	Arginine ADP-ribosylation mechanism based on structural snapshots of iota-toxin and actin complex. Proceedings of the National Academy of Sciences of the United States of America, 2013, 110, 4267-4272.	7.1	73
9	The catalytic mechanism of dyeâ€decolorizing peroxidase DyP may require the swinging movement of an aspartic acid residue. FEBS Journal, 2011, 278, 2387-2394.	4.7	72
10	Identification of 16 novel mutations in the argininosuccinate synthetase gene and genotype-phenotype correlation in 38 classical citrullinemia patients. Human Mutation, 2003, 22, 24-34.	2.5	71
11	Clostridium perfringens lota-Toxin: Structure and Function. Toxins, 2009, 1, 208-228.	3.4	64
12	The calcium-binding property of equine lysozyme. FEBS Letters, 1987, 223, 405-408.	2.8	63
13	Sequential Aldol Condensation Catalyzed by Hyperthermophilic 2-Deoxy- <scp>d</scp> -Ribose-5-Phosphate Aldolase. Applied and Environmental Microbiology, 2007, 73, 7427-7434.	3.1	62
14	Structural basis of d-DOPA oxidation by d-amino acid oxidase: Alternative pathway for dopamine biosynthesis. Biochemical and Biophysical Research Communications, 2007, 355, 385-391.	2.1	61
15	Role of Sphingomyelinase in Infectious Diseases Caused by Bacillus cereus. PLoS ONE, 2012, 7, e38054.	2.5	59
16	Nucleolin as cell surface receptor for tumor necrosis factor-α inducing protein: a carcinogenic factor of Helicobacter pylori. Journal of Cancer Research and Clinical Oncology, 2010, 136, 911-921.	2.5	52
17	Human Dâ€amino acid oxidase: an update and review. Chemical Record, 2007, 7, 305-315.	5.8	49
18	The First Crystal Structure of Hyperthermostable NAD-dependent Glutamate Dehydrogenase from Pyrobaculum islandicum. Journal of Molecular Biology, 2005, 345, 325-337.	4.2	47

#	Article	IF	CITATIONS
19	Crystal structures of dyeâ€decolorizing peroxidase with ascorbic acid and 2,6â€dimethoxyphenol. FEBS Letters, 2012, 586, 4351-4356.	2.8	43
20	The First Crystal Structure of Archaeal Aldolase. Journal of Biological Chemistry, 2003, 278, 10799-10806.	3.4	42
21	Calcium-Binding Lysozymes. Biological Chemistry Hoppe-Seyler, 1988, 369, 671-676.	1.4	41
22	Crystal structure of the ADP-dependent glucokinase from Pyrococcus horikoshii at 2.0-Ã resolution: A large conformational change in ADP-dependent glucokinase. Protein Science, 2009, 11, 2456-2463.	7.6	40
23	Crystal Structure of a Novel FAD-, FMN-, and ATP-containing l-Proline Dehydrogenase Complex from Pyrococcus horikoshii. Journal of Biological Chemistry, 2005, 280, 31045-31049.	3.4	39
24	Crystal Structure of the NAD Biosynthetic Enzyme Quinolinate Synthase. Journal of Biological Chemistry, 2005, 280, 26645-26648.	3.4	36
25	Structural analysis of human glutamine:fructoseâ€6â€phosphate amidotransferase, a key regulator in type 2 diabetes. FEBS Letters, 2009, 583, 163-167.	2.8	29
26	X-ray Structure of a Pokeweed Antiviral Protein, Coded by a New Genomic Clone, at 0.23 nm Resolution. A Model Structure Provides a Suitable Electrostatic Field for Substrate Binding. FEBS Journal, 1994, 225, 369-374.	0.2	26
27	Clostridium perfringens \hat{I}^1 -toxin, ADP-ribosyltransferase: structure and mechanism of action. Advances in Enzyme Regulation, 2003, 43, 361-377.	2.6	26
28	Nucleotide sequence of a genomic gene encoding tritin, a ribosome-inactivating protein from Triticum aestivum. Plant Molecular Biology, 1993, 22, 171-176.	3.9	25
29	A second novel dye-linked L-proline dehydrogenase complex is present in the hyperthermophilic archaeon Pyrococcus horikoshii OT-3. FEBS Journal, 2005, 272, 4044-4054.	4.7	25
30	Crystallization and Preliminary X-ray Crystallographic Studies of Recombinant Human Leukotriene A4 Hydrolase Complexed with Bestatin. Journal of Molecular Biology, 1994, 238, 854-856.	4.2	24
31	Structural Basis for the Kexin-like Serine Protease from Aeromonas sobria as Sepsis-causing Factor. Journal of Biological Chemistry, 2009, 284, 27655-27663.	3.4	24
32	Rho GTPase Recognition by C3 Exoenzyme Based on C3-RhoA Complex Structure. Journal of Biological Chemistry, 2015, 290, 19423-19432.	3.4	24
33	Comparative study of the stability of the folding intermediates of the calciumâ€binding lysozymes. International Journal of Peptide and Protein Research, 1993, 41, 118-123.	0.1	23
34	Cryo-EM structures reveal translocational unfolding in the clostridial binary iota toxin complex. Nature Structural and Molecular Biology, 2020, 27, 288-296.	8.2	21
35	A structural study of calcium-binding equine lysozyme by two-dimensional 1H-NMR. BBA - Proteins and Proteomics, 1991, 1078, 77-84.	2.1	18
36	Structure of l-aspartate oxidase from the hyperthermophilic archaeon Sulfolobus tokodaii. Biochimica Et Biophysica Acta - Proteins and Proteomics, 2008, 1784, 563-571.	2.3	18

#	Article	IF	CITATIONS
37	Structural basis for the Helicobacter pylori-carcinogenic TNF-α-inducing protein. Biochemical and Biophysical Research Communications, 2009, 388, 193-198.	2.1	16
38	Crystal structure of archaeal highly thermostable <scp>L</scp> â€aspartate dehydrogenase/NAD/citrate ternary complex. FEBS Journal, 2007, 274, 4315-4325.	4.7	14
39	<i>Anabaena</i> sp. DyP-type peroxidase is a tetramer consisting of two asymmetric dimers. Proteins: Structure, Function and Bioinformatics, 2016, 84, 31-42.	2.6	14
40	Substrate N2 atom recognition mechanism in pierisin family DNA-targeting, guanine-specific ADP-ribosyltransferase ScARP. Journal of Biological Chemistry, 2018, 293, 13768-13774.	3.4	13
41	Chondroitin Sulfate Proteoglycan Is a Potent Enhancer in the Processing of Procathepsin L. Biological Chemistry, 2002, 383, 1925-9.	2.5	11
42	Structure of a Hyperthermophilic Archaeal Homing Endonuclease, I-Tsp0611: Contribution of Cross-domain Polar Networks to Thermostability. Journal of Molecular Biology, 2007, 365, 362-378.	4.2	11
43	Nonâ€native αâ€helix formation is not necessary for folding of lipocalin: Comparison of burstâ€phase folding between tear lipocalin and Î²â€łactoglobulin. Proteins: Structure, Function and Bioinformatics, 2009, 76, 226-236.	2.6	11
44	Crystal structure of the YdjC-family protein TTHB029 from Thermus thermophilus HB8: Structural relationship with peptidoglycan N-acetylglucosamine deacetylase. Biochemical and Biophysical Research Communications, 2008, 367, 535-541.	2.1	10
45	Refolding, characterization and crystal structure of (S)-malate dehydrogenase from the hyperthermophilic archaeon Aeropyrum pernix. Biochimica Et Biophysica Acta - Proteins and Proteomics, 2009, 1794, 1496-1504.	2.3	10
46	Presence of a Motif Conserved between Helicobacter pylori TNFALPHA. Inducing Protein (Tip.ALPHA.) and Penicillin-Binding Proteins. Biological and Pharmaceutical Bulletin, 2005, 28, 2133-2137.	1.4	9
47	Structural Basis of Free Reduced Flavin Generation by Flavin Reductase from Thermus thermophilus HB8. Journal of Biological Chemistry, 2011, 286, 44078-44085.	3.4	9
48	Common Mechanism for Target Specificity of Protein- and DNA-Targeting ADP-Ribosyltransferases. Toxins, 2021, 13, 40.	3.4	9
49	Crystal structure and structure-based mutagenesis of actin-specific ADP-ribosylating toxin CPILE-a as novel enterotoxin. PLoS ONE, 2017, 12, e0171278.	2.5	9
50	Crystallization and preliminary X-ray crystallographic analysis of Mirabilis antiviral protein. Journal of Molecular Biology, 1992, 226, 281-283.	4.2	8
51	Structure and stability of Gyuba, a Î²â€łactoglobulin chimera. Protein Science, 2011, 20, 1867-1875.	7.6	8
52	Reaction Mechanism of Mono-ADP-Ribosyltransferase Based on Structures of the Complex of Enzyme and Substrate Protein. Current Topics in Microbiology and Immunology, 2014, 384, 69-87.	1.1	8
53	Conformational plasticity is crucial for C3-RhoA complex formation by ARTT-loop. Pathogens and Disease, 2015, 73, ftv094.	2.0	8
54	Conformational Polymorphism of m7GTP in Crystal Structure of the PB2 Middle Domain from Human Influenza A Virus. PLoS ONE, 2013, 8, e82020.	2,5	8

#	Article	IF	CITATIONS
55	Crystallization and X-ray diffraction analysis of the RNA primer/promoter-binding domain of influenza A virus RNA-dependent RNA polymerase PB2. Acta Crystallographica Section F: Structural Biology Communications, 2009, 65, 144-146.	0.7	7
56	Structural Basis for Action of the External Chaperone for a Propeptide-deficient Serine Protease from Aeromonas sobria. Journal of Biological Chemistry, 2015, 290, 11130-11143.	3.4	7
57	Crystallization and Preliminary X-Ray Studies of the Ia Component of Clostridium perfringens Iota Toxin Complexed with NADPH. Journal of Structural Biology, 1999, 126, 175-177.	2.8	6
58	Substrate selectivity of bacterial monoacylglycerol lipase based on crystal structure. Journal of Structural and Functional Genomics, 2014, 15, 83-89.	1.2	6
59	Comparative Studies of Actin- and Rho-Specific ADP-Ribosylating Toxins: Insight from Structural Biology. Current Topics in Microbiology and Immunology, 2016, 399, 69-86.	1.1	6
60	The carboxyâ€ŧerminal tail of <i>Aeromonas sobria</i> serine protease is associated with the chaperone. Microbiology and Immunology, 2009, 53, 647-657.	1.4	5
61	Role of side-edge site of sphingomyelinase from Bacillus cereus. Biochemical and Biophysical Research Communications, 2012, 422, 128-132.	2.1	5
62	Precipitant-Free Lysozyme Crystals Grown by Centrifugal Concentration Reveal Structural Changes. Crystal Growth and Design, 2018, 18, 4226-4229.	3.0	5
63	Structure of an archaeal alanine:glyoxylate aminotransferase. Acta Crystallographica Section D: Biological Crystallography, 2008, 64, 696-699.	2.5	4
64	Crystallization and preliminary X-ray diffraction studies of a surface mutant of the middle domain of PB2 from human influenza A (H1N1) virus. Acta Crystallographica Section F, Structural Biology Communications, 2014, 70, 72-75.	0.8	3
65	Involvement of the Arg566 residue of Aeromonas sobria serine protease in substrate specificity. PLoS ONE, 2017, 12, e0186392.	2.5	3
66	Crystallization and preliminary X-ray crystallographic studies of monoacylglycerol lipase of the moderately thermophilicBacillussp. H-257. Acta Crystallographica Section D: Biological Crystallography, 2002, 58, 1232-1233.	2.5	2
67	Crystallization and preliminary X-ray diffraction analysis of homing endonuclease I-Tsp0611. Acta Crystallographica Section D: Biological Crystallography, 2004, 60, 2006-2008.	2.5	2
68	The first crystal structure of an archaeal helical repeat protein. Acta Crystallographica Section F: Structural Biology Communications, 2005, 61, 636-639.	0.7	2
69	Crystallization and preliminary X-ray diffraction analysis of glutamate dehydrogenase from an aerobic hyperthermophilic archaeon, Aeropyrum pernix K1. Acta Crystallographica Section D: Biological Crystallography, 2002, 58, 1338-1339.	2.5	1
70	Crystallization and preliminary X-ray diffraction analysis of the hyperthermostable NAD-dependent glutamate dehydrogenase fromPyrobaculum islandicum. Acta Crystallographica Section D: Biological Crystallography, 2004, 60, 715-717.	2.5	1
71	Enteric Toxins of Clostridium perfringens. , 2015, , 997-1013.		1
72	A myelin sheath protein forming its lattice. Journal of Biological Chemistry, 2020, 295, 8706-8707.	3.4	1

#	Article	IF	CITATIONS
73	Preparation of Clostridium perfringens binary iota-toxin pore complex for structural analysis using cryo-EM. Methods in Enzymology, 2021, 649, 125-148.	1.0	1
74	1P030 Molecular Mechanism of Actin Recognition by Arginine ADP-ribosylating Toxin(Proteins-functions, methodology, and protein enigineering,Oral Presentations). Seibutsu Butsuri, 2007, 47, S31.	0.1	0
75	3P-004 Crystal structure of influenza virus RNA polymerase PB2 including host determinant residue K627(Protein:Structure,The 47th Annual Meeting of the Biophysical Society of Japan). Seibutsu Butsuri, 2009, 49, S151.	0.1	0
76	Crystal Structure and Function of Actin-Specific ADP Ribosyl Toxin Seibutsu Butsuri, 2003, 43, 168-173.	0.1	0
77	Cryo-EM Structural Analysis of Binary Toxin:. Nihon Kessho Gakkaishi, 2022, 64, 69-76.	0.0	0